

# Meridional Propagation of Zonal Jets in Ocean Gyres

B.T. NADIGA AND D.N. STRAUB

## 1.1 Introduction

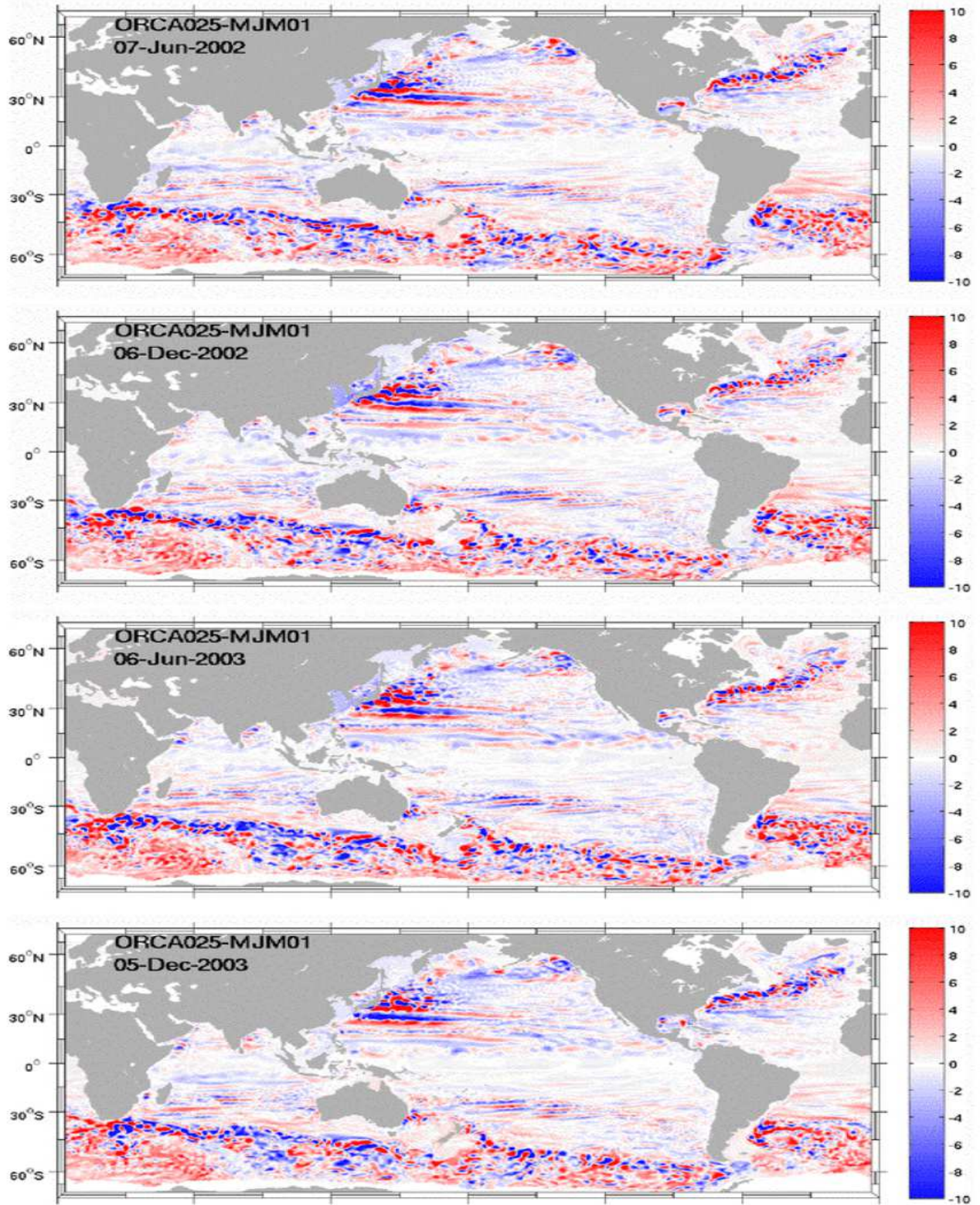
Analyses of both altimetric data and in-situ measurements reveal patterns of meridionally-alternating, nearly zonal, coherent jet-like structures in many of the world ocean basins (Maximenko et al., 2005, 2008; Ivanov et al., 2009; Melnichenko et al., 2010; van Sebillie et al., 2011). A number of realistic Ocean General Circulation Model (OGCM) simulations also display similar structures (e.g. Treguier et al., 2003; Nakano and Hasumi, 2005; Richards et al., 2006). Most such analyses, whether model- or altimetry-based, consider averages, typically over several months, of geostrophic velocity. Generally, these jet-like structures i) extend zonally from just a few degrees to tens of degrees of longitude, ii) display meridional wavelengths in the range of one to as many as five degrees of latitude, iii) show a high degree of vertical coherence, and iv) have speeds of a few centimeters per second. In many instances, the jet orientation is slightly off-zonal. For brevity we will refer to these structures as alternating zonal jets, or simply, jets.

It has been suggested that the jets may be simple artifacts of averaging over westward propagating eddies (e.g., Schlax and Chelton, 2008). More commonly, the jets are assumed not to be artifacts, and many dynamical formation mechanisms have been put forth. For example, alternating jets are well-known from  $\beta$ -plane turbulence and are associated with a halting of the two-dimensional inverse energy cascade by Rossby wave dispersion (e.g., Rhines, 1975; Vallis and Maltrud, 1993). It is thus possible that the observed alternating jets in the oceans are a result of the anisotropic inverse cascade mechanism (Kramer et al., 2006; Nadiga, 2006). They may also result from nonlinear self-interactions of linear eigenmodes (Berloff et al., 2009) or from radiating instabilities of unstable eastern boundary currents (Hristova et al., 2008; Wang et al., 2012). They may be related to preferred growing structures excited by the imposed stochastic forcing (Farrell and Ioannou, 2007; Bakas and Ioannou, 2013) or be manifestations of the  $\beta$ -plume effect (e.g. Afanasyev et al., 2012). Finally, it has been suggested that the jets might be formed by an instability of Rossby waves (Lorenz, 1972; Gill, 1974; Connaughton et al., 2010). As with altimetry-based and realistic OGCM-based analyses of the jets, most of the process studies that motivate these various formation mechanisms also consider temporal averages of geostrophic velocity anomalies. Additionally, issues related to meridional

propagation of the jets is generally not emphasized, and is explicitly treated only in the last set of studies (which considers the formation of zonal and off-zonal jet structures in the context of Rossby wave instability). It is also only in this set of studies that issues of off-zonality are explicitly considered.

The recent analysis by Penduff (2008) of one of his OGCM simulations is one case in which off-zonal orientation and meridional propagation are seen. In one of his climatology-forced ocean/sea-ice simulations—ORCA025-MJM01, an animation of the 18 month-running average of SSH over a dozen years makes evident the propagating nature of alternating jets that form in his simulations (Penduff, 2008). In recent quasigeostrophic (QG) simulations of wind driven gyres, we have found jets be near-ubiquitous and to propagate in a manner similar to Penduff’s animation. In the QG simulations, both the jets and their propagation are clearly visible in the instantaneous fields—without the need for time averaging. They are especially clear in snapshots of the baroclinic zonal velocity, for example. Given that the propagating nature of the jets and their presence in instantaneous snapshots of model simulations has not yet received much attention, we focus on these aspects of alternating jets for most of this chapter. We will also comment on the formation mechanism in our two layer quasigeostrophic  $\beta$ -plane simulations. Specifically, we will consider whether the jets might be formed via an instability Rossby waves, which are also ubiquitous in our simulations.

Connaughton et al. (2010) consider modulational instability of Rossby waves in the barotropic and equivalent-barotropic settings, extending the analysis of Gill (1974). For weak waves ( $M = \psi_0 p^3 / \beta \ll 1$  where  $\psi_0$  is the initial amplitude of the Rossby wave of wavenumber  $p$  and  $\beta$  is the usual meridional gradient of Coriolis frequency), they show that maximum growth occurs for off-zonal modulations that are close to being in three-wave resonance with the primary wave. For strong waves ( $M \gg 1$ ), the most unstable modes are perpendicular to the primary wave. For a strong primary wave having a zonally-oriented wavevector, the growing modes thus have meridionally-oriented wavevectors ( $k_x = 0$ ), corresponding to zonal flow. Note also that the Rossby wave dispersion relation ( $\omega = -\beta k_x / (k^2 + L_d^{-2})$ )—where  $\omega$  is the wave frequency,  $k_x$  is the zonal wavenumber,  $k$  is the total horizontal wavenumber and  $L_d$  is the Rossby deformation radius—then has that jets excited by this mechanism would be steady. On the other hand, when the primary Rossby wave is weak, off-zonality of the unsta-



ble mode leads to propagation of the off-zonal jets, again due to nature of the dispersion relation.

**Figure 1.1** Snapshots from the Penduff (2008) animation mentioned in the text. Time increases from top to bottom in 26 week intervals; focusing attention on the meridional position of the jets in successive snapshots shows a clear meridional propagation.

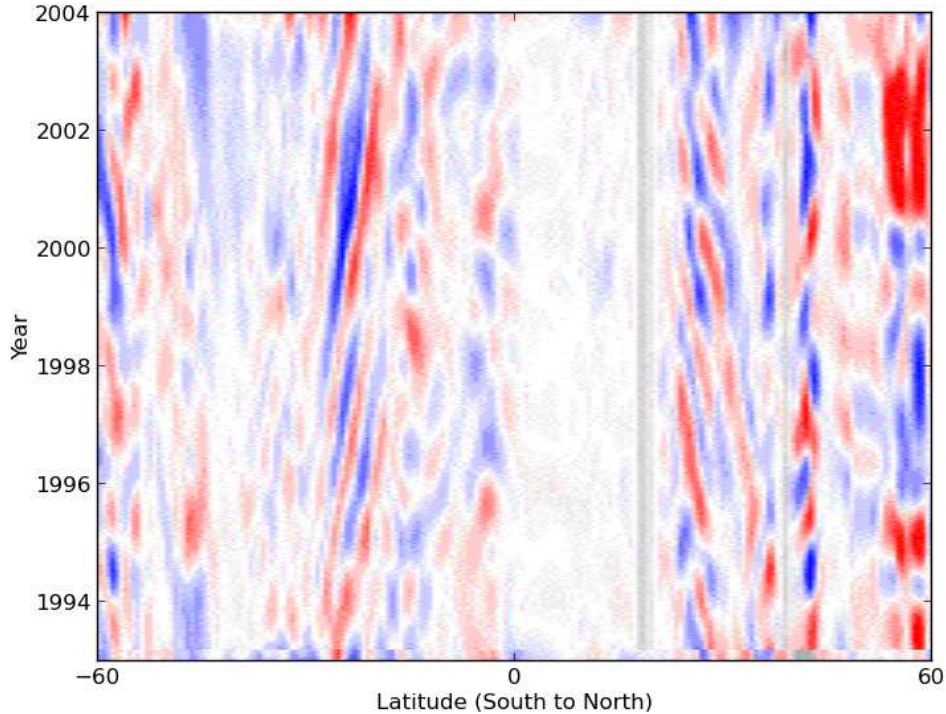


**Figure 1.2** Hovmöller plots in the western Pacific from Penduff’s animation. Equatorward propagation of jets in sub-tropical gyres (around 30 degrees North and South) is evident; the rate of propagation is roughly about one degree of latitude per year. There are also hints of poleward propagation of the jets in the North Pacific sub-polar gyre (around 60 degrees North).

The Rossby wave instability mechanism discussed above is independent of the source of the primary Rossby waves, which could be triggered by any number of processes. For example, in the oceanic context, long baroclinic Rossby waves can be radiated from the eastern boundary, either due to unstable boundary currents there (as, e.g., in Hristova et al., 2008; Wang et al., 2012) or due to energy arriving there in the form of Kelvin waves. In a multi-layer QG basin, mass conservation leads to a parameterization of Kelvin waves that determines the value of baroclinic streamfunctions on the basin perimeter. This can lead to oscillations in the value of the streamfunction (equivalently, the thermocline height) along the boundary, and these oscillations can excite Rossby waves. In particular, long Rossby waves generated in this way are commonly seen propagating westward from the eastern boundary in quasigeostrophic gyre simulations. In our QG simulations, we also see barotropic Rossby waves, as well as a band of Rossby-wave-like features that have a mixed baroclinic-barotropic character and lie adjacent to the region populated by jets.

Nadiga and Straub (2010) considered the barotropic  $\beta$ -plane vorticity equation in a closed basin with steady double gyre forcing and found the spontaneous appearance of alternating jets in long time averages. The jets were associated with a weakly-forced, weakly-dissipated limit, and also evident in this limit was a “double cascade” of energy. That is, the upscale nonlinear transfer (familiar from classic studies of 2-dimensional turbulence) was offset by a forward transfer due to the  $\beta$  term. That the linear  $\beta$  term could transfer energy at all is related to the basin geometry; in a periodic setting, this term is not directly associated with energy transfer between scales. Straub and Nadiga (2014) considered the two-layer double gyre problem and

also found both quasi-zonal jets and a double cascade of barotropic energy. They did not emphasize the jets or find any clear link between their characteristics and the double cascade. They did, however, find the jets to be present over a wide range of parameters and to be easily visible in snapshots of the baroclinic streamfunction. Aspects of the jets in this baroclinic QG double gyre setting will be discussed in Section 3.

## 1.2 Alternating jets in a $\frac{1}{4}^\circ$ OGCM Simulation

Penduff et al. (2010) considered global ocean/sea-ice simulations driven by realistic atmospheric forcing over the period 1993-2004. They considered four horizontal resolutions ( $2^\circ$ ,  $1^\circ$ ,  $\frac{1}{2}^\circ$ , and  $\frac{1}{4}^\circ$ ) and compared sea level anomalies (SLA) against the AVISO SLA dataset. In various measures, they found a monotonic improvement in the comparison with resolution. In conjunction with their  $\frac{1}{4}^\circ$  simulation, they also conducted a companion simulation—ORCA025-MJM01. The only difference with this simulation was that it was forced by an annually-repeating average of the atmospheric forcing fields Penduff (2008). The reader is referred to Penduff (2008) for an animation of the 18-month running average of SSH in this companion run. In this animation, the



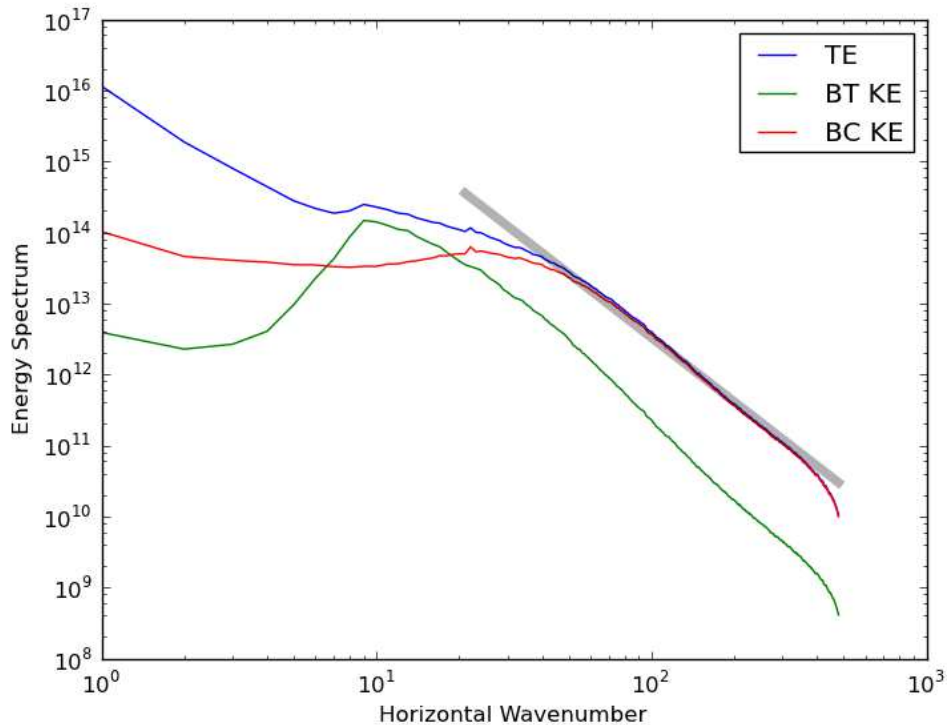


**Figure 1.3** Time-averaged spectra of barotropic and baroclinic kinetic energy and of total energy for our reference QG simulation.

propagating nature of the alternating jets is evident in the subtropical and subpolar gyres of the North Pacific and in the supolar gyre of the South Pacific. For reference, Fig. 1.1 shows four snapshots from that animation of sea surface height (SSH) separated by 26 weeks each. Not only is the widespread appearance of alternating banded structures evident in these snapshots, but the propagation of these structures may be surmised by focusing attention on their meridional location in the successive snapshots going from top to bottom.

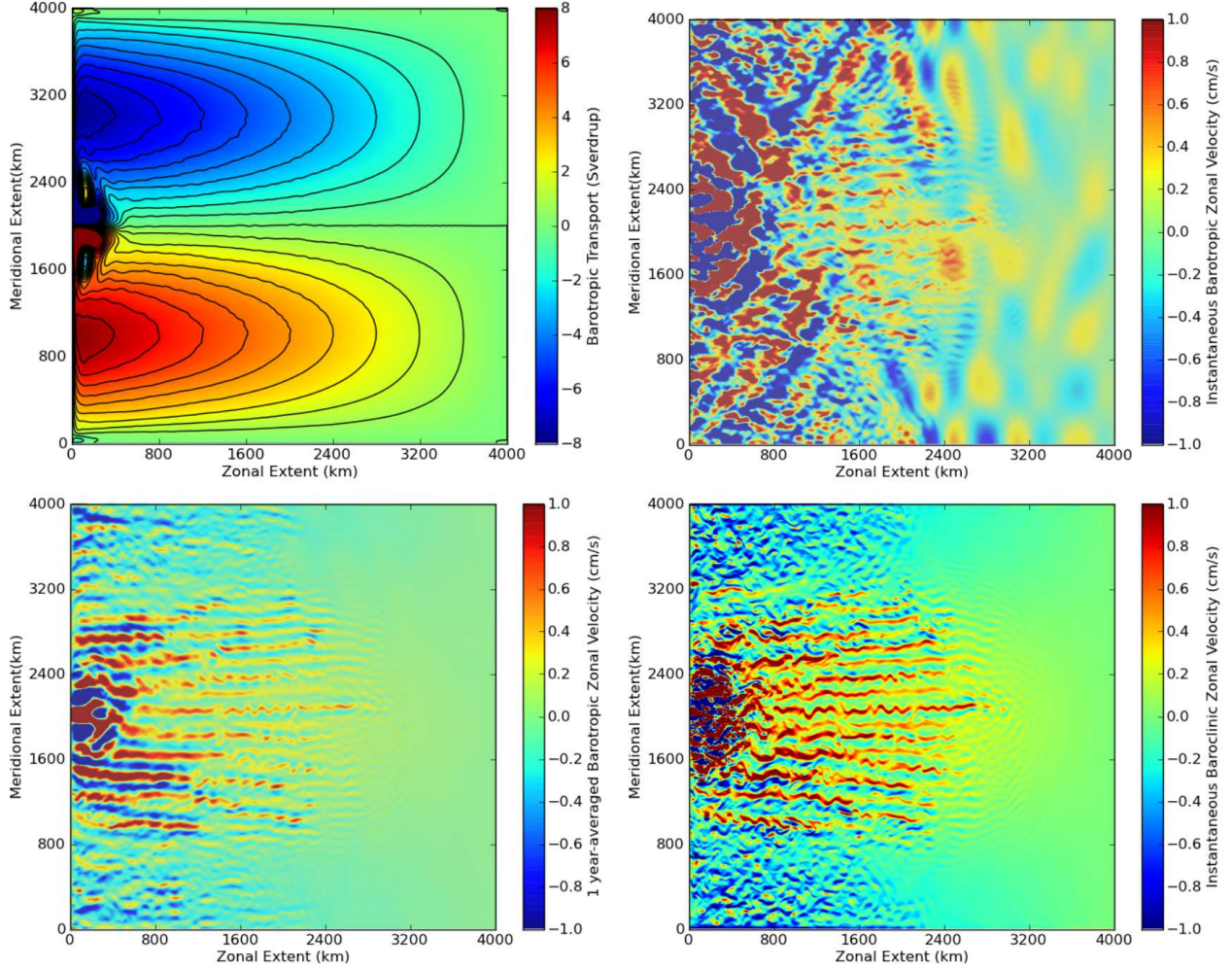
To better demonstrate this propagation, Fig. 1.2 shows the time evolution of SSH as a Hovmöller diagram. In this diagram, the equatorward propagation of the alternating jets in the northern and southern subtropical gyres (around  $\pm 30^\circ$ ) is evident. There are also further hints of poleward propagation of similar structures in the northern subpolar gyre, with the Antarctic Circumpolar Current complicating the picture in the south. In the subpolar gyres, the alternating jets are seen to propagate at speeds of roughly one degree of latitude per year.

### 1.3 Jets in the QG double gyre problem

We have found alternating zonal jets to be a near-ubiquitous feature of two layer QG double gyre simulations over a wide range of deformation radii and forcing and dissipation parameters. The jets are easily visualized as quasi-zonal structures in the instantaneous zonal velocity associated with the baroclinic mode. They are also evident in snapshots of the barotropic zonal velocity, although in this case larger scale structures are superposed on the jets. The character of the

jets varies somewhat with parameters; it is particularly sensitive to the deformation radius, for example. Simulations assuming a large deformation radius show the central jet stemming from the confluence of the two western boundary currents to be relatively strong, with the alternating jets being fewer and less pronounced. For small deformation radii, the converse is true, and the alternating jets are particularly robust. Forcing and dissipation strengths also affect the jets. The jet region is bounded to the east, north, and south by a band wavelike features, and this band is more pronounced in weakly forced or strongly damped (bottom friction) simulations. We will consider later whether this band of waves might play a role in establishing the jets or whether it might instead be thought of as modified Rossby waves that propagate away from the jet region. Since the jets are particularly evident in low deformation radius simulations, we will first consider this case ( $L_d = 15$  km; referred to as our reference case). We then present results from simulations a) that use a larger deformation radius ( $L_d = 30$  km) and b) that use a weaker wind forcing as compared to the reference run.

We emphasize that the jets appearing in this two-layer setting owe their existence to an interaction involving both layers; equivalently, involving both the barotropic and baroclinic modes. As mentioned above, in other work we have also found alternating jets in barotropic double gyre simulations; however, in the single layer setting, the jets are weak and are visible only in long time averages. Similarly, a reduced gravity version of the barotropic equations does not produce jets that are visible in snapshots. It thus seems that the jets in a two-layer setting are somehow fundamen-



tally related to an interaction between the barotropic and baroclinic modes.

We consider the quasigeostrophic equations truncated to two layers in the vertical. Written in the layer form, the governing equations are

$$\begin{aligned} \frac{\partial q_i}{\partial t} + J(\psi_i, q_i) + \beta v_i &= \delta_{i1} F - \delta_{i2} r \nabla^2 \psi_i + A \nabla^8 \psi_i \\ q &= \nabla^2 \psi_i + (-1)^i \frac{f_0^2}{g' h_i} (\psi_1 - \psi_2) \end{aligned} \quad (1.1)$$

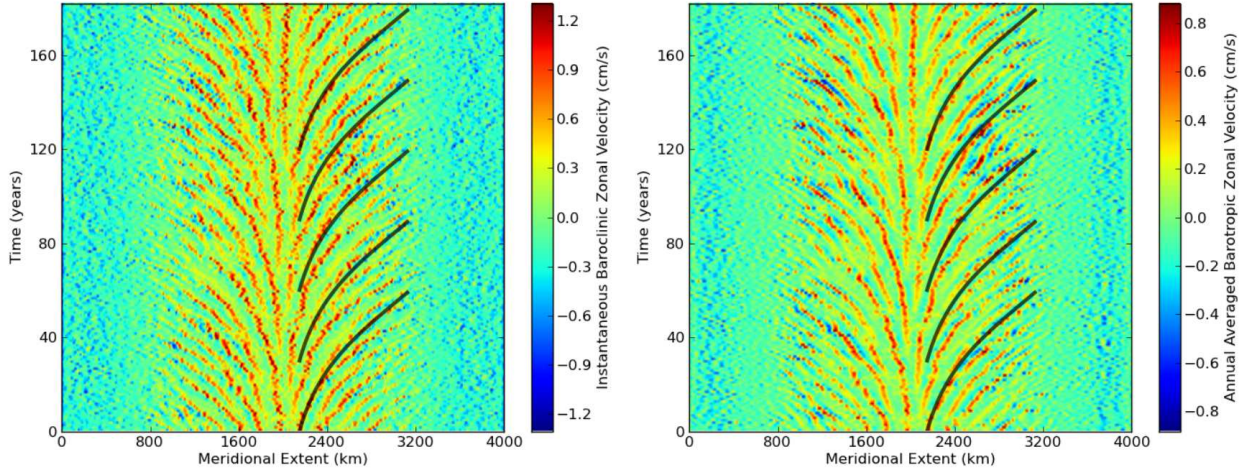
In the above equations, besides the standard notation used, the subscript  $i$  is the layer index: 1 for upper, 2 for lower,  $q$  is quasigeostrophic potential vorticity (QGPV),  $\psi$  is streamfunction,  $J(\psi_i, q_i) = \partial \psi_i / \partial x \partial q_i / \partial y - \partial \psi_i / \partial y \partial q_i / \partial x$  and represents horizontal advection of QGPV, and  $\delta_{ij} = 1$  if  $i = j$  and 0 otherwise (implying that the wind forcing is applied only to the upper layer and bottom friction to the lower layer). These equations are solved in a closed mid-latitude  $\beta$ -plane domain that is discretized on a regular Cartesian grid. For the biharmonic viscosity used, boundary conditions consisted of setting both relative vorticity and its Laplacian to zero at the horizontal boundary. A nominally fifth order adaptive time-stepping Runge-Kutta Cash-Karp method was used for time integration and a direct solve was

**Figure 1.4** Physical space fields for our reference simulation: Sixty year time average of barotropic streamfunction (upper left), instantaneous snapshot of the barotropic zonal velocity (upper right), one year average of the barotropic zonal velocity (lower left), instantaneous snapshot of the baroclinic zonal velocity (lower right).

used for inverting the quasigeostrophic potential vorticity-streamfunction equation.

We revisit the classic baroclinic wind-driven double gyre problem. The domain consists of a 4000 km square  $\beta$ -plane basin with upper and lower layer thicknesses of 1 km and 4 km, respectively. The horizontal domain is spanned by 960 points in each direction to yield a horizontal grid spacing  $\Delta x \approx 4.2$  km. The reference simulation uses a first internal Rossby deformation radius of 15 km. A steady sinusoidal double gyre windstress with a maximum amplitude of  $0.1 \text{ Nm}^{-2}$  is applied to the upper layer. The reference drag coefficient is set to  $10.67 \times 10^{-8} \text{ s}^{-1}$ . A biharmonic form of horizontal dissipation was used to dissipate the forward-cascading potential enstrophy; the coefficient of this biharmonic viscosity was chosen to scale as  $A = \beta \Delta x^5$ , with  $\beta = 2 \times 10^{-11} \text{ m}^{-1} \text{ s}^{-1}$ . This choice allows for a smooth tapering of the energy spectra at high wavenumber, and is sufficiently small such that dissipation due to the biharmonic





term is small. The one dimensional horizontal spectra of barotropic and baroclinic kinetic energy, total energy, and a reference  $-3$  slope are shown in Fig. 1.3.

Figure 1.4 shows various physical space fields for our reference simulation. The long-time ( $\approx 180$  year) average (upper left) of the barotropic streamfunction shows the double gyre structure, with an approximate Sverdrup balance (e.g. Pedlosky, 1987) over most of the domain. Also evident, near the western boundary, are tight inertial recirculations. These are confined to a region close to the boundary; this apparently being a consequence of the relatively small deformation radius (for larger deformation radii, these recirculations extend farther east; not shown). There is no clear evidence of jets in the long-time average. By contrast, the instantaneous barotropic velocity (upper right) does show evidence of jets. Superposed on the jets are larger scale diagonally-oriented features that appear to be barotropic Rossby waves; they do not appear in the baroclinic mode and animations show them to propagate rapidly with westward phase velocities. Similar wave structures also obscure the jets in the upper layer velocity field. Time averaging serves to remove these structures (lower left panel), so that the jets can be more easily visualized. We emphasize that time averaging makes the jets visible by removing structures superposed on the jets; it is not the case that the jets result from time averaging of propagating eddies. Put another way, the jets can also be made more evident by a spatial filtering of snapshots, without the need for time averaging (not shown). By contrast, no such filtering (in space or time) is needed to make the jets evident in the baroclinic mode. Instead, in the baroclinic mode, the jets are clearly visible in unprocessed snapshots (lower right panel).

From visual inspection, it appears that the barotropic and baroclinic jets evident in snapshots are related. Moreover, animations show the jets associated with each mode to propagate outward from the center latitude at comparable speeds. This propagation is also evident in Fig. 1.5, which shows Hovmoller plots of two of the fields depicted in Fig. 1.4. Jets appear to form near the center latitude and propagate meridionally outwards. Note that the propagation speed is latitude-dependent, being fastest near the (latitudinal) centers of the two gyres (e.g., near 1000 or

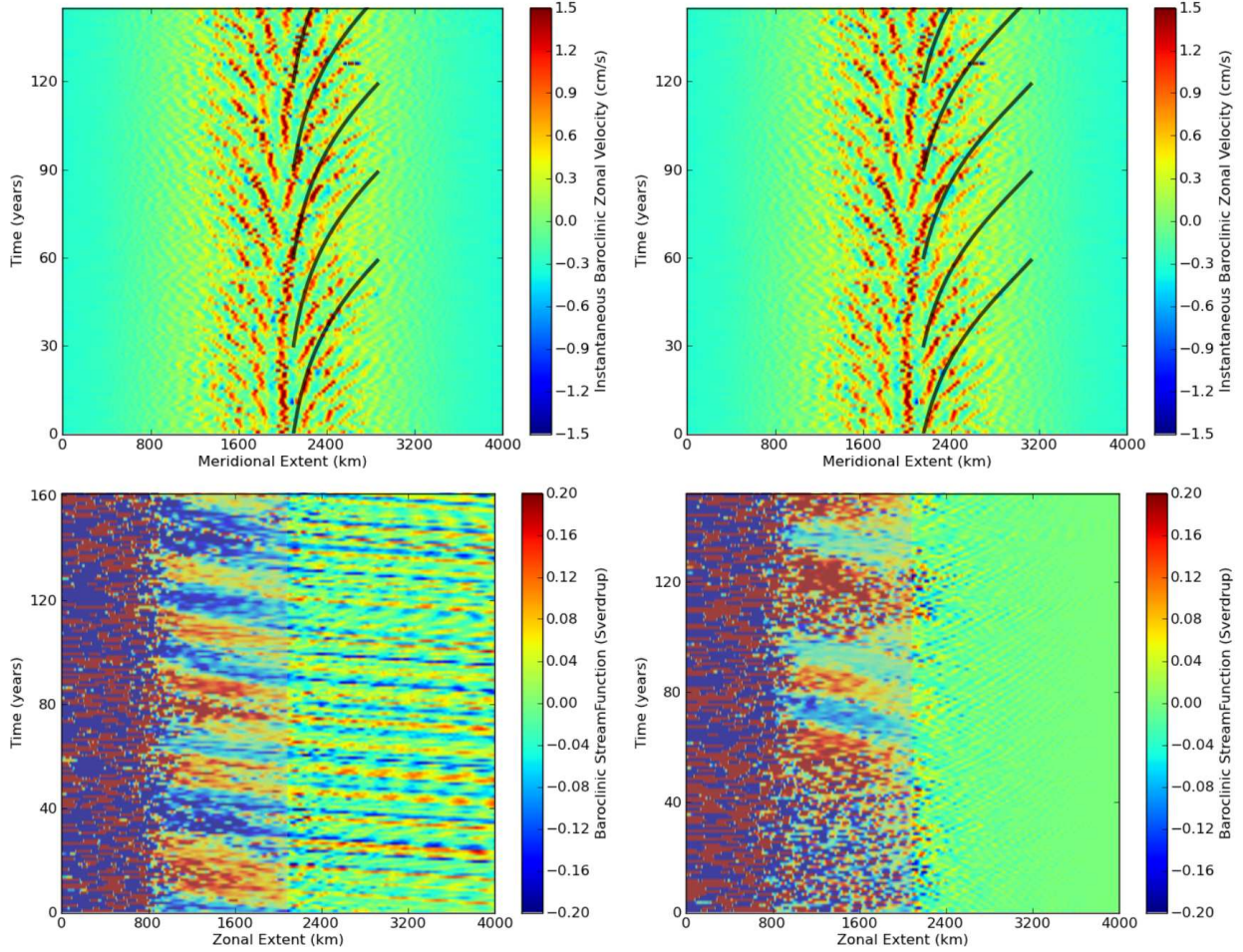
**Figure 1.5** Hovmoller plots of instantaneous baroclinic (left) and one year-averaged barotropic (right) zonal velocities for our reference simulation. The zonal location considered is 1600 km from the western boundary. The jets are seen to slowly propagate equatorward in the sub-tropical gyre and poleward in the sub-polar gyre. Reference black curves drawn are propagated outwards from the central latitude by the time-mean baroclinic meridional velocity.

3000 km on the horizontal axes in Fig. 1.5). This suggests that the propagation speed might scale with the meridional component of the Sverdrup velocity, which also peaks at these same latitudes. The curves overlain in Fig 1.5 emphasize this point. Plotted is a family of curves,  $y(t)$ . Each curve begins at a small distance,  $y_0$ , north of the center latitude and obeys  $dy/dt = v_{BC}(y)$ , where  $v_{BC}$  is the time averaged baroclinic meridional velocity, or about twice the depth-averaged meridional velocity.<sup>1</sup> The curves fit reasonably well with the observed propagation. Exactly why this should be the case remains unclear. The figure does provide clear evidence, though, that the meridional propagation of the jets is in large part due to advection by the gyres.

The top left panel of Fig. 1.6 is analogous to the left panel in Fig. 1.5, but for a more realistic value of the deformation radius ( $L_d = 30$  km; all other parameters are as in our reference simulation). As anticipated, jets are wider and fewer when the deformation radius is increased. Also as anticipated, meridional propagation is also evident here. The overlain curves are analogous to those in Fig. 1.5. Although the fit is less impressive than before, there nonetheless remains the suggestion that advection by the gyres plays a key role in the meridional propagation.

The bottom left panel in Fig. 1.6 is an  $x$ - $t$  Hovmoller plot of the baroclinic streamfunction. It shows a broad pattern of westward propagation extending back from about  $x = 2000$  km. This appears to be low frequency Rossby waves, possibly generated by the break-up of the midlatitude jet at about this same longitude. Note also the clear signature of westward propagating long Rossby waves stemming from the

<sup>1</sup> The linear modes are normalized such that  $\psi_{\text{barotropic}} = \epsilon_1 \psi_1 + \epsilon_2 \psi_2$  and  $\psi_{\text{baroclinic}} = \epsilon_3 (\psi_1 - \psi_2)$ , where  $\epsilon_1$  and  $\epsilon_2$  are the fractional layer thicknesses (here 0.2 and 0.8, respectively), and  $\epsilon_3 = (\epsilon_1 \epsilon_2)^{1/2}$ .



eastern boundary. As mentioned in the introduction, it is possible that the jets are formed in association with an instability of these waves. Indeed, O'Reilly et al. (2012) found that addition of a fast time scale stochastic single-gyre forcing to the classic double gyre problem resulted in robust long Rossby waves; and related to these, jets. In our simulations, the forcing is steady and the Rossby waves are instead formed in association with a lifting and lowering of the wall value for the baroclinic streamfunction. That is, at each time step a function,  $\tau(x, y)$ , must be added to the potential-vorticity-containing part of the baroclinic streamfunction. The function  $\tau(x, y)$  obeys

$$\nabla^2 \tau - \frac{1}{L_d^2} \tau = 0 \quad (1.2)$$

with  $\tau = \tau_0$  on the boundary. Here,  $\tau_0$  is chosen such that the area integral of  $\tau$  is equal and opposite to that of the potential-vorticity-containing part of the baroclinic streamfunction. The spatial structure of  $\tau$  is that it decays over a distance  $L_d$  from its value on the perimeter to a value of zero in the interior. Typically  $\tau_0$  varies with time, and this lifting and lowering of the thermocline excites Rossby waves.

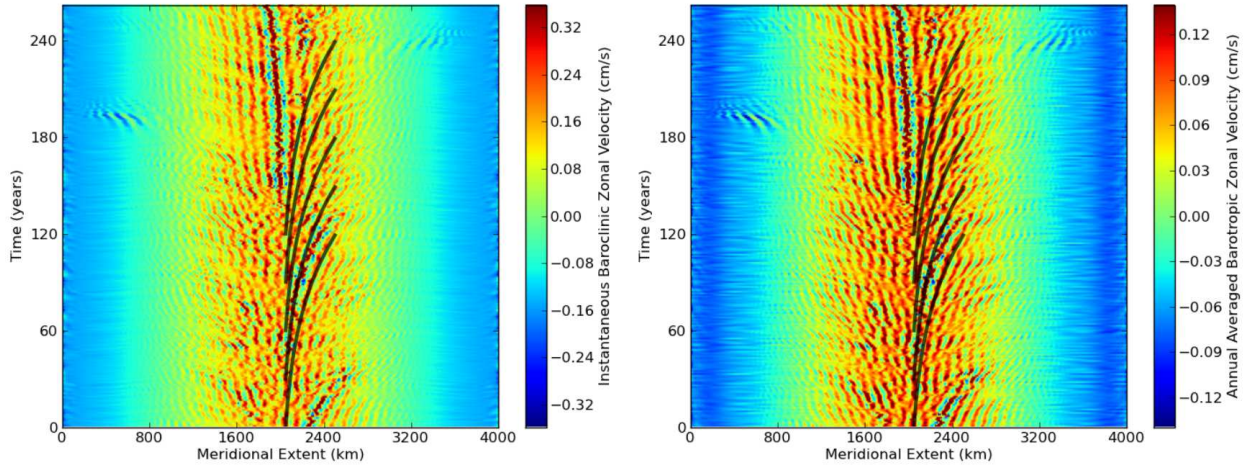
To test whether an instability of these long Rossby waves might be central to the formation of the jets, we ran a companion simulation in which this zero potential vorticity mode was artificially suppressed (i.e.,  $\tau_0$  was set to zero). The right

**Figure 1.6** Hovmöller diagrams for our 30 km deformation radius simulation. Upper panels are as in the left panel of Fig. 1.5. Lower panels plot the instantaneous baroclinic streamfunction at  $y = 2000$  km and show zonal propagation. Left panels keep the wall mode ( $\tau$ ) and right panels do not (i.e., the right panels are for a companion simulation in which  $\tau$  was artificially set to zero at each time step). A “waterstain” has been added to the left side of the lower panels for added visual clarity.

panels of Fig. 1.6 are analogous to the left ones, but for the companion simulation. Clearly, this suppression filters the long Rossby waves emanating from the eastern boundary, but does not filter the jets. Both the jets and their meridional propagation persist in the absence of these long Rossby waves; in fact, the two upper panels suggest that the jets are virtually unaltered when the wall mode is suppressed. This was also the case in our 15 km simulation; although there, the long Rossby waves (present when the zero potential vorticity was retained) were weaker and associated with a lower band of frequencies. Additionally, snapshots of the baroclinic zonal velocity were virtually indistinguishable between cases where the zero potential vorticity mode was kept and those where it was not. We thus conclude that the jets are not formed in association with instability of Rossby waves generated at the eastern boundary.

Figure 1.7 shows Hovmöller diagrams analogous to those in Fig. 1.5, but for a simulation forced by weak winds (max-





imum stress of  $0.05 \text{ Nm}^{-2}$  as opposed to  $0.1 \text{ Nm}^{-2}$  for our reference simulation). As before, the plots are scaled so as to emphasize the jets. This scaling makes not only the jets, but also the zonal velocity associated with the gyres evident. Such was not the case in Fig. 1.5. In other words, relative to the gyres, the jets are weaker here. Also as before, curves indicative of advection by the baroclinic Sverdrup velocity are overlain. The fit of these curves with the jets near the center latitude is quite good; however, it is less good near the center of the gyres, where  $v_{BC}$  is maximal and, at times, the jets appear to stall. Further out from the center (e.g., around  $y = 3000 \text{ km}$  in the north or  $y = 1000 \text{ km}$  in the south) lies a band of wavelike structures. This can be seen by enlarging Fig. 1.7, but is blurred in the print version. Wave bursts sometimes appear (e.g., around days 180 and 240 in Fig. 1.7) and produce packets that propagate outward from the jet region. More typically, these wavelike features remain adjacent to the jet region. A physical space picture is given in Fig. 1.8. Plotted is the instantaneous baroclinic speed for our weak wind simulation, scaled so as to make this relatively weak band of wavelike structures more evident. A similar waveband is also seen in the barotropic mode and an outward group velocity can be inferred from a Hovmöller diagram (not shown); the outward group velocity suggest that it is more natural to think of these features as excited by the jet-turbulence region, rather than as playing a significant role in forming the jets.

In the introduction, we mentioned the possibility that the jets may be formed by an instability of Rossby waves. We have seen four types of waves or wavelike features evident in our simulations. These are a) the band of mixed barotropic-baroclinic waves discussed above, b) the long baroclinic Rossby waves stemming from the eastern boundary, c) the barotropic Rossby waves (e.g., evident in the upper right panel of Fig. 1.4) and d) the broad baroclinic westward propagation extending back from near the eastern edge of the jet region (e.g., lower panels of Fig. 1.6). We have also presented evidence that the first two are not likely responsible for forming the jets. The barotropic waves, present whether or not the wall mode is kept) may be involved in an instability leading to the jets; unfortunately, we had no simple way to filter them, and so were not able to test this numer-

**Figure 1.7** Similar to Fig.1.5, but for our weakly forced simulation. The alternating zonal jets are seen to get weaker with respect to the gyre circulation when the windstress reduced by a factor of 2. The meridional propagation also slows down, suggesting that it is related to advection by the Sverdrup velocity.

ically. The broad westward propagation back from near the center longitude of the basin (d, above) is the least well-characterized of these four types. These features appear to form near the eastern extent of the jet region and propagate back towards the west. This suggests that their dynamics are somehow linked to those of the jets. On one hand, they appear to be formed by the jets; on the other, they propagate back into the jet region, and hence may be involved in sustaining the jets, once formed.

## 1.4 Conclusions

In this chapter, we have emphasized the meridional propagation of jets embedded in mid-latitude ocean gyres. We also emphasized that the jets are clearly evident in snapshots, particularly of the baroclinic mode. The meridional propagation seems related to an advective mechanism. In particular, the propagation speed appears to agree well with the baroclinic gyre velocity. The agreement is not perfect. Also, why the advecting velocity should be  $v_{BC}$  (equivalently, twice the depth-averaged Sverdrup velocity) is unclear. What forms the jets also remains unclear. Jets evident in snapshots do not appear in barotropic or single layer reduced gravity simulations, suggesting that their formation is somehow fundamentally related to an interaction between the barotropic and baroclinic modes. In the introduction, we mentioned formation mechanisms involving instabilities of Rossby waves. In simulations not presented here, we have also seen jets to be formed by similar instability mechanisms. For example, artificially lifting and lowering the thermocline height along the boundary (i.e.,  $\tau_0$ ) produces Rossby waves that propagate inward from the basin boundaries. Simulations driven solely by this mechanism (i.e., with no potential vorticity



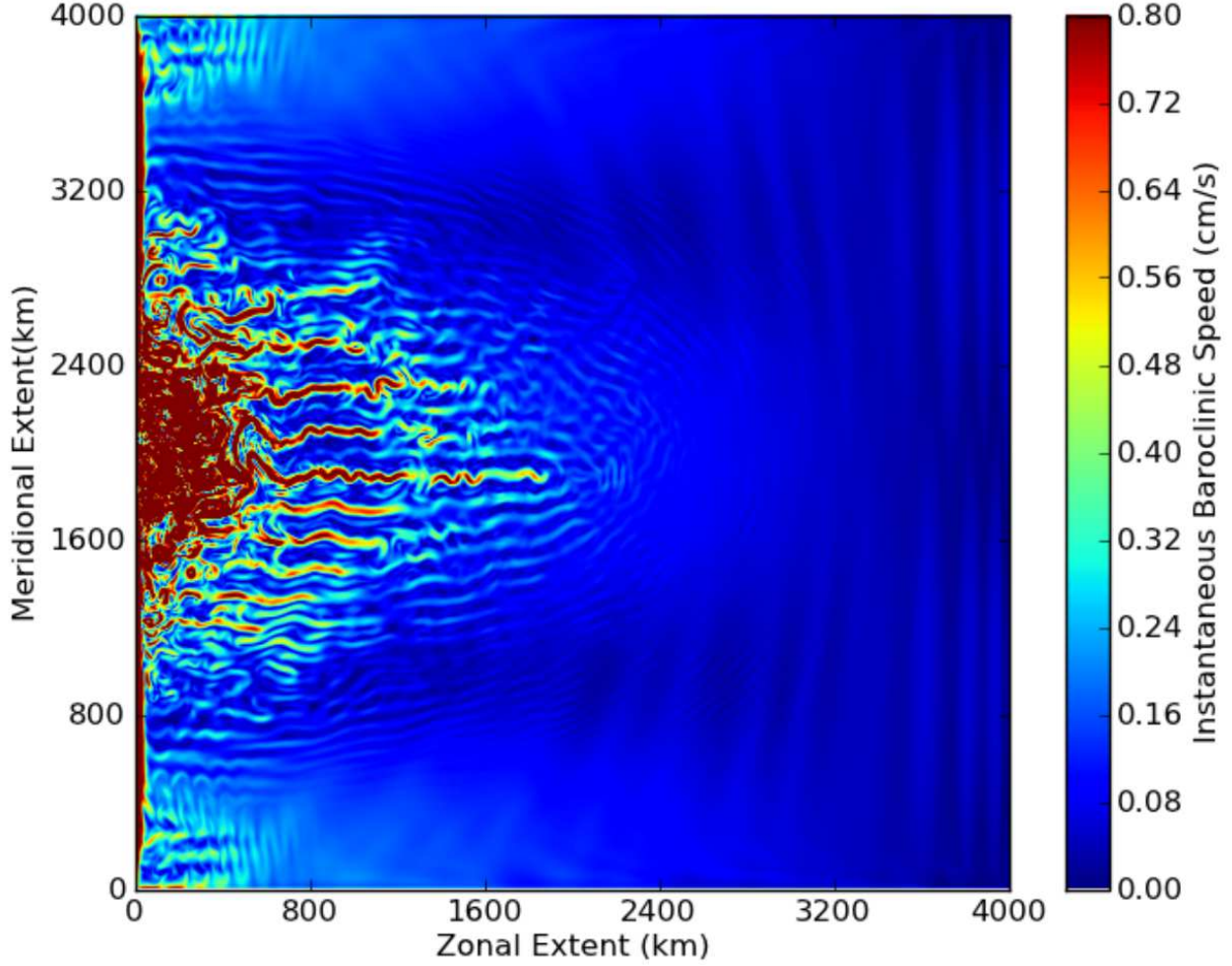


**Figure 1.8** Baroclinic speed for our weakly forced simulation. Values have been capped so as to emphasize the band of short Rossby waves surrounding the jet region.

forcing at all) can produce wave trains that go unstable to form zonal jets. This occurs, however, only when the forcing is sufficiently strong. In our wind-driven gyre simulations, the Rossby waves generated naturally by this dynamics are relatively weak, and this does not appear to be the mechanism responsible for the jets seen in these simulations. For example, artificially suppressing the wall mode produced jets that were virtually indistinguishable from those in simulations where this wall mode was kept. In other periodic two-layer simulations (also not presented), we have seen short Rossby waves go unstable to produce, at least temporarily, jet-like features. Our gyre simulations do show the presence of short Rossby-wave-like features surrounding the jet region. These waves are of a mixed barotropic-baroclinic nature and appear to be associated with eastward group velocities. As such, it seems more natural to interpret them as produced by the turbulent dynamics of the boundary current confluence region. Consistent with this idea, these waves are energetically weak.

Having ruled out a number of formation mechanisms, we note that a hypothesis that we are currently investigating is that the jets result from an instability of the main eastward flow associated with the confluence of the subtropical and subpolar gyres. Since individual jets can typically be traced (e.g., using animations or Hovmöller plots) back to

near the center jet, it seems likely that the jets form as an instability of this “main jet”. In more realistic simulations (such as the Penduff simulations highlighted in section 2), this would correspond to the eastward extension of, say, the Gulf Stream or Kuroshio. It may be possible to understand the weaker, alternating, jets seen on either side of these major currents as resulting from an instability (perhaps involving waves propagating through the region) of these major currents.

# REFERENCES

- Afanasyev, YD, O’leary, S, Rhines, PB, and Lindahl, E. 2012. On the origin of jets in the ocean. *Geophysical & Astrophysical Fluid Dynamics*, **106**(2), 113–137.
- Bakas, Nikolaos A, and Ioannou, Petros J. 2013. On the Mechanism Underlying the Spontaneous Emergence of Barotropic Zonal Jets. *Journal of the Atmospheric Sciences*, **70**(7).
- Berloff, P, Kamenkovich, I, and Pedlosky, J. 2009. A mechanism of formation of multiple zonal jets in the oceans. *Journal of Fluid Mechanics*, **628**, 395.
- Connaughton, Colm P, Nadiga, Balasubramanya T, Nazarenko, Sergey V, and Quinn, Brenda E. 2010. Modulational instability of Rossby and drift waves and generation of zonal jets. *Journal of Fluid Mechanics*, **654**, 207.
- Farrell, Brian F, and Ioannou, Petros J. 2007. Structure and spacing of jets in barotropic turbulence. *Journal of the Atmospheric Sciences*, **64**(10), 3652–3665.
- Gill, AE. 1974. The stability of planetary waves on an infinite beta-plane. *Geophysical and Astrophysical Fluid Dynamics*, **6**(1), 29–47.
- Hristova, Hristina G, Pedlosky, Joseph, and Spall, Michael A. 2008. Radiating instability of a meridional boundary current. *Journal of Physical Oceanography*, **38**(10), 2294–2307.
- Ivanov, LM, Collins, CA, and Margolina, TM. 2009. System of quasi-zonal jets off California revealed from satellite altimetry. *Geophysical Research Letters*, **36**(3).
- Kramer, Werner, van Buren, MG, Clercx, HJH, and van Heijst, GJF. 2006.  $\beta$ -plane turbulence in a basin with no-slip boundaries. *Physics of Fluids*, **18**(2), 026603–026603.
- Lorenz, Edwadd N. 1972. Barotropic instability of Rossby wave motion. *J. Atm. Sci.*, **29**.
- Maximenko, Nikolai A, Bang, Bohyun, and Sasaki, Hideharu. 2005. Observational evidence of alternating zonal jets in the world ocean. *Geophysical research letters*, **32**(12), L12607.
- Maximenko, Nikolai A, Melnichenko, Oleg V, Niiler, Pearn P, and Sasaki, Hideharu. 2008. Stationary mesoscale jet-like features in the ocean. *Geophysical Research Letters*, **35**(8), L08603.
- Melnichenko, Oleg V, Maximenko, Nikolai A, Schneider, Niklas, and Sasaki, Hideharu. 2010. Quasi-stationary striations in basin-scale oceanic circulation: vorticity balance from observations and eddy-resolving model. *Ocean Dynamics*, **60**(3), 653–666.
- Nadiga, Balasubramanya T. 2006. On zonal jets in oceans. *Geophysical research letters*, **33**(10).
- Nadiga, BT, and Straub, DN. 2010. Alternating zonal jets and energy fluxes in barotropic wind-driven gyres. *Ocean Modelling*, **33**(3), 257–269.
- Nakano, Hideyuki, and Hasumi, Hiroyasu. 2005. A series of zonal jets embedded in the broad zonal flows in the Pacific obtained in eddy-permitting ocean general circulation models. *Journal of physical oceanography*, **35**(4), 474–488.
- O’Reilly, Christopher H, Czaja, Arnaud, and LaCasce, JH. 2012. The emergence of zonal ocean jets under large-scale stochastic wind forcing. *Geophysical Research Letters*, **39**(11).
- Pedlosky, Joseph. 1987. *Geophysical fluid dynamics*. 2nd edn. Springer-Verlag.
- Penduff, T, Juza, M, Brodeau, L, Smith, G C, Barnier, B, Molines, J-M, Treguier, A-M, and Madec, G. 2010. Impact of global ocean model resolution on sea-level variability with emphasis on interannual time scales. *Ocean Science Discussions*, **6**, 269–284.
- Penduff, Thierry. 2008. *Forced and intrinsic ocean interannual variability (1993-2004)*. [http://lgge.osug.fr/meom/pages-perso/Thierry/Francais/en\\_animations.html](http://lgge.osug.fr/meom/pages-perso/Thierry/Francais/en_animations.html), accessed: 2013-12-03.
- Rhines, Peter B. 1975. Waves and turbulence on a beta-plane. *J. Fluid Mech*, **69**(3), 417–443.
- Richards, KJ, Maximenko, NA, Bryan, FO, and Sasaki, H. 2006. Zonal jets in the Pacific Ocean. *Geophysical research letters*, **33**(3).
- Schlax, Michael G, and Chelton, Dudley B. 2008. The influence of mesoscale eddies on the detection of quasi-zonal jets in the ocean. *Geophysical Research Letters*, **35**(24).
- Straub, David N, and Nadiga, Balasubramanya T. 2014. Energy Fluxes in the Quasigeostrophic Double Gyre Problem. *Journal of Physical Oceanography*, **44**(6), 1505–1522.
- Treguier, AM, Hogg, NG, Maltrud, M, Speer, K, and Thierry, V. 2003. The Origin of Deep Zonal Flows in the Brazil Basin\*. *Journal of physical oceanography*, **33**(3), 580–599.
- Vallis, Geoffrey K, and Maltrud, Matthew E. 1993. Generation of mean flows and jets on a beta plane and over topography. *Journal of physical oceanography*, **23**(7), 1346–1362.
- van Seille, Erik, Kamenkovich, Igor, and Willis, Josh K. 2011. Quasi-zonal jets in 3-D Argo data of the northeast Atlantic. *Geophysical Research Letters*, **38**(2), L02606.
- Wang, Jinbo, Spall, Michael A, Flierl, Glenn R, and Malanotte-Rizzoli, Paola. 2012. A new mechanism for the generation of quasi-zonal jets in the ocean. *Geophysical Research Letters*, **39**(10).